DEVELOPMENT OF HIGH FIELD DIPOLE AND HIGH CURRENT PULSE POWER SUPPLY FOR COMPACT PROTON SYNCHROTRON

K. Endo and K. Egawa, KEK & SKD, Tsukuba, Japan

Z. Fang, NIRS & KEK, Chiba, Japan

M.Mizobata and A. Teramoto, Mitsubishi Electric Corp., Kobe, Japan

Abstract

A small dipole magnet of 3 T is developed with its pulse power supply feeding 200 kA at maximum for the table-top proton synchrotron which is now under development for the radiotherapy. The experimental field distribution is consistent with the 3D dynamic field simulation results satisfying the required beam aperture. The dipole field was measured at an interval of 2 msec with 15 tiny search coils aligned accurately to the radial direction in the pole gap. The dipole is excited by the discharge current of the capacitor bank of 53 kJ with the rise time of 5 msec. Transverse beam behavior is also simulated using a time dependent beam optics code under the influence of the RF acceleration field to estimate the required beam apertures. Performances of the dipole and power supply will be treated in detail in conjunction with the numerical simulations.

INTRODUCTION

In order to make the proton synchrotron of 200 MeV for the radiation therapy small enough for installation and daily clinical treatment in the hospital environment, the development of the high field compact dipole magnet with performance of the accelerator grade is indispensable [1, 2]. The pioneering work has been initiated at BINP using a compact electron synchrotron model ring which was followed by the development of a small 5 T dipole magnet with a small beam aperture [3, 4]. Another requirement to the compact ring is to reduce the overall longitudinal dimension of the RF cavity with the average accelerating gradient of ~40 kV/m [5]. Its RF frequency range is well wide and the accelerating voltage is very large to accomplish the acceleration within duration while the ohmic heat dissipation can allow the temperature rise of the dipole coil. The RF issues are treated by the paper of this conference [6].

According to the size of the horizontal beam aperture, the cross-sectional dimensions of the dipole become large. If they are limited by the ring size, the iron core saturation becomes large when attaining a high magnetic field. There is a room for a trade off between the maximum field strength and the beam aperture. The present optics design has a preference to the beam aperture so as to obtain the sufficient beam intensity extracted for the medical treatment. The peak field of the dipole is suppressed to 3 T at 200 MeV, however, the dipole core saturates considerably.

The pulse power supply was also manufactured. It depends on the charge/discharge of the energy storage capacitor and the discharge current steps up through the pulse transformer to attain the peak current of 200 kA corresponding to the dipole field of 3 T. The power supply and the dipole magnet compose a resonant circuit of which rise time is used for the acceleration [7].

RING PARAMETERS

Main machine parameters are tabulated in Table 1 and the present ring layout is shown in Fig.1. Each design has the different dispersion and the horizontal/vertical tunes depending on the cell structure. The present design adopts the triplet cell structure to decrease the dispersion at the dipole magnet.

Table 1: Parameters for a 200 MeV proton synchrotron.

|	BINP	BINP-Frascati	KEK	unit
Max. energy	200.0	200.0	200.0	MeV
Inj. energy	1.0	12.0	2.0	MeV
Circumference	4.7	6.4	11.9	m
Av. diameter	1.5	2.0	3.6	m
Bending radius	0.43	0.54	0.72	m
Max. dipole field	5.0	4.0	3.0	T
Period	4	4	4	
Tune, Q_x/Q_y	1.4/0.45	1.42/0.54	2.25/1.25	
Max. dispersion	0.4	0.63	0.5	m
Cell structure	FODB	BODO	FODOFB	
Frequency range	4.16~36.1	7.4~26.5	1.86~16.2	MHz
Acc. voltage	11.5	12.4	13.0	kV
Acc. time	2.5	3.5	5.0	msec
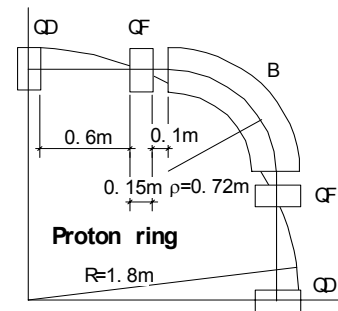
Figure 1: Layout of the compact proton synchrotron.

DIPOLE MAGNET

The ring consists of 4 dipole magnets. One of them was manufactured as a model according to the design (Fig.2) by the time dependent 3D field simulation (Fig.3). Both ends of the pole extending 5 cm from the core edges are tapered to attain a uniform effective dipole length as

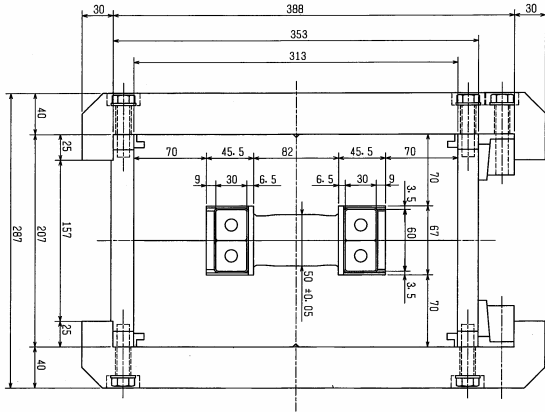shown in Fig.4 and the completed dipole magnet is given in Fig.5.

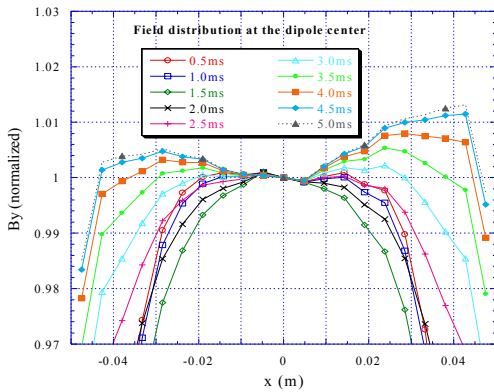Figure 2: Cross-sectional dimensions of the dipole.

Figure 3: Field distribution at the dipole center without correction windings at every 0.5 msec.
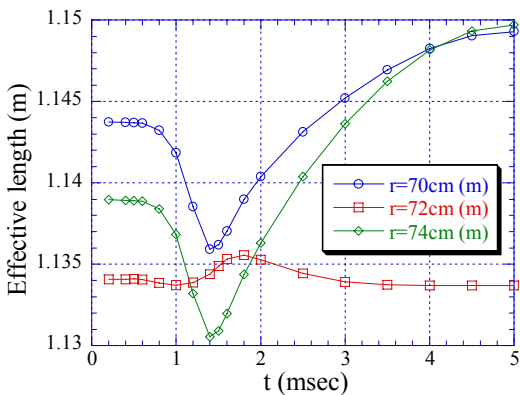

Figure 4: Numerically obtained effective length as a function of time. The squares correspond to the central orbit.

The field distribution is measured by using 15 search coils precisely aligned to the radial direction in the probe holder which are moved manually at every 0.9 or 0.45 deg. step on the girder. Induced voltage is saved at every 2 µsec and integrated to convert it to the field data in the personal computer. The normalized distribution at the center of the dipole is given in Fig.6 which reproduces the

numerically obtained distribution of Fig.3. The effective magnet length along the central orbit is given in Fig.7. At low field the effective length is longer by about 20 mm than the simulation. The time base differs somewhat in Fig.6 and Fig.7 where the maximum field is 2.94 T at 5.56 msec.
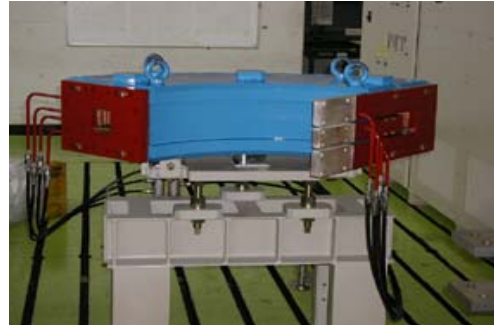

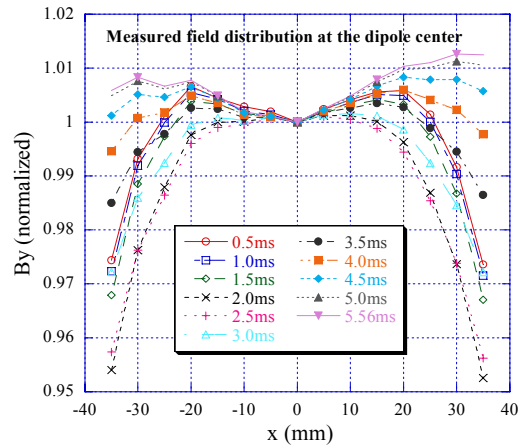Figure 5: Completed dipole magnet.
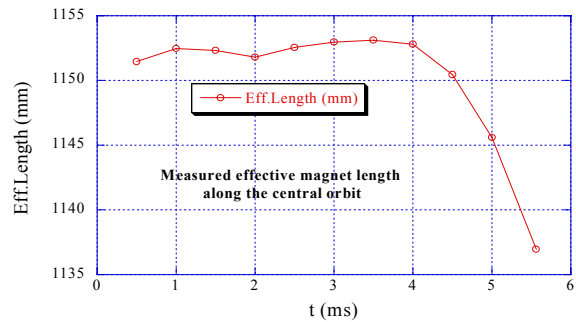

Figure 6: Measured field distributions.

Figure 7: Measured effective magnet length.

The effective magnet length is obtained by integrating numerically the measured field map of the gap medium plane. As the search coil moves on the circular arc both inside and outside of the dipole, the outside integration on the tangential line (Fig.8) was made of the interpolated field, which is calculated by the method of the iso-parametric transformation in conjunction with the generalized matrix inversion.

PULSE POWER SUPPLY

By the thermal restraint, the current pulse width should be short. Assuming the sinusoidal excitation with a peak current I_p and a pulse rate η repetitions/sec, the effective current is $I_{eff} = 0.5 I_p \sqrt{\eta / f}$ for the rise and fall time equivalent to f Hz. This case is $I_{eff} = 14.1 \sqrt{\eta}\ [kA]$. In practice, the current differs from the sinusoidal pattern due to the saturation of the dipole magnet and the repetition rate is 5 or less depending on the heat dissipation. To avoid the skin effect the coil is made of the strand Cu cable impregnated with the epoxy resin of which heat conductivity is considerably small.
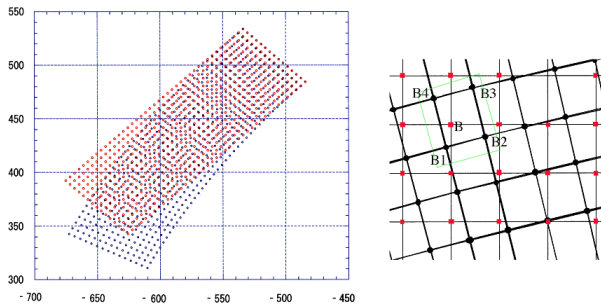

Figure 8: Interpolation of the magnetic field. (Left) Blue spots: the measured field points, and red spots: interpolated if surrounded by 4 blue points. (Right) A red point field is interpolated from 4 black point data in a green rectangle.

As the discharge current of the capacitor bank is utilized to excite the dipole, the precise current control is difficult. However, the precise tracking of the quad current must be established by sensing the dipole current or field which is the reference signal to the quad power supplies. This kind of control is easy because the current of these quad power supplies is about one tenth of the dipole current.

The power supply shown in Fig.9 has the capacitor bank (2.5 mF, 6.5 kV) to excite one dipole.

Before manufacturing the pulse power supply, the charge, discharge and residual energy recovery circuits are simulated using PSpice code for all dipoles serially connected. The current pulse width is adjusted to 10 msec (50 Hz equivalent) by changing the circuit parameters such as the pulse transformer winding ratio, capacitor, charging voltage and etc. The measured current pulse and the central dipole field are plotted in Fig.10 when the energy recovery circuit is working.

Figure 9: Completed pulse power supply for a dipole magnet. From left to right; charge, control, capacitor bank and discharge blocks.
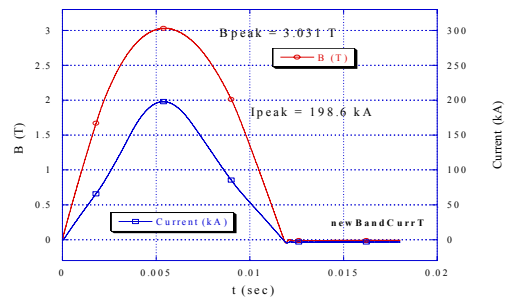

Figure 10: Measured time-dependent excitation curve.

REFERENCES

[1] K. Endo et al, "Table-Top Proton Synchrotron Ring for Medical Applications," Proc. EPAC2000, Wien, pp.2515-7.

[2] K. Endo et al, "Compact Proton and Carbon Ion Synchrotron for Radiation Therapy," Proc. EPAC2002, Paris, 2733-5.

[3] I.I. Averbukh et al, "Project of Small-Dimensional 200 MeV Proton Synchrotron," EPAC88, Rome, 1988, pp.413-6.

[4] L. Picardi et al, "Preliminary Design of a Very Compact Protosynchrotron for Proton Therapy," EPAC94, 1994, pp.2607-9.

[5] Z. Fang et al, "A Broadband and High Gradient RF Cavity for a Compact Proton Synchrotron," Proc. EPAC2002, Paris, pp.2145-7.

[6] Z. Fang et al, "RF Cavities and Power Amplifier for the Compact Proton Synchrotron," this conference.

[7] K. Endo et al, "Resonant Pulse Power Supply for Compact Proton and/or Heavy Ion Synchrotron," Proc. APAC2001, Beijing, pp.636-8.